Check for updates

A Maitake (*Grifola frondosa*) polysaccharide ameliorates Alzheimer's disease-like pathology and cognitive impairments by enhancing microglial amyloid-β clearance

Yao Bai, [ID] †[a] Lingling Chen,†[a] Yao Chen,[a] Xinmeng Chen,[b] Yilong Dong,[a] Shangyong Zheng,[a] Lei Zhang,[c] Weiyuan Li,[a] Jing Du*[a] and Hongliang Li [ID] *[a]

Alzheimer's disease (AD) is characterized by the deposition of amyloid-β (Aβ) plaques, neuronal loss and neurofibrillary tangles. In addition, neuroinflammatory processes are thought to contribute to AD pathophysiology. Maitake (*Grifola frondosa*), an edible/medicinal mushroom, exhibits high nutritional value and contains a great amount of health-beneficial, bioactive compounds. It has been reported that proteo-β-glucan, a polysaccharide derived from Maitake (PGM), possesses strong immunomodulatory activities. However, whether PGM is responsible for the immunomodulatory and neuroprotection effects on APP$_{swe}$/PS1$_{\Delta E9}$ (APP/PS1) transgenic mice, a widely used animal model of AD, remains unclear. In the present study, the results demonstrated that PGM could improve learning and memory impairment, attenuate neuron loss and histopathological abnormalities in APP/PS1 mice. In addition, PGM treatment could activate microglia and astrocytes and promote microglial recruitment to the Aβ plaques. Also, PGM could enhance Aβ phagocytosis, and thereby alleviate Aβ burden and the pathological changes in the cortex and hippocampus in APP/PS1 mice. Moreover, PGM showed no significant effect on mice body weight. In conclusion, these findings indicated that administration of PGM could improve memory impairment *via* immunomodulatory action, and dietary supplementation with PGM may provide potential benefits on brain aging related memory dysfunction.

Introduction

Alzheimer's disease (AD) is the most common neurodegenerative disease and accounts for the most common cause of amnesia in the aging population.[1] It is estimated that close to 150 million people worldwide are affected by AD, which causes an enormous financial burden on the family and society.[2,3] Despite remarkable progress in understanding the pathophysiology of AD, current pharmacotherapeutic options are still very limited. Therefore, it is necessary for us to find suitable medication to prevent the onset of AD and delay its progression.

It has been reported that amyloid-β (Aβ) aggregation and deposition is a critical early event in the pathogenesis of AD that initiates a cascade of events including neuronal dysfunction, tau aggregation and hyperphosphorylation, and neuronal

death.[1,4] Aβ accumulation has been demonstrated to result from an imbalance between Aβ production and clearance in the brain. There is growing evidence that impaired clearance of Aβ is responsible for the most common type of AD.[5,6] Therefore, to redress the imbalance of Aβ homeostasis and remove the overproduction of Aβ plaques from the brain might be effective strategies to counteract AD. Microglia and astrocytes are two major types of glial cells involved in regulation of neuro-inflammation and deposition of Aβ. Microglia are thought to regulate the degree of Aβ deposition by phagocytosis of Aβ aggregates with potentially protective impact on AD progression.[7,8] Besides providing beneficial effects to the host, chronic activation of microglial also led to an overproduction of neurotoxic inflammatory cytokines and reactive oxygen species.[9] Taken together, it remains unclear if microglia have a net protective or harmful effect, and the precise mechanisms by which microglia alter the course of AD neuropathology remain poorly understood. Therefore, it is imperative to elucidate how microglia are involved in Aβ clearance and characterize their roles in the disease progression of AD.

As an alternative and complementary therapy, functional foods have been attracted a great deal of attention in recent years. It has been suggested that some functional foods may be

[a] School of Medicine, Yunnan University, 2 Cuihu North Road, Kunming, 650091, People Republic of China. E-mail: dujing@ynu.edu.cn; lihongliang@ynu.edu.cn; Fax: +86-871-65034358; Tel: +86-871-65034358

[b] School of Biomedical Sciences, The Chinese University of Hong Kong, Shatin, NT Hong Kong, People Republic of China

[c] School of Basic Medicine, Yunnan University of Chinese Medicine, 1076 Yuhua Road, Kunming, 650500, People Republic of China

† These authors contributed equally to this work.

target candidates for treating AD.[10,11] For example, ginger and aged garlic extract have been found to be effective in the treatment for AD-related amnesia and neurodegenerative disorders.[10,12] Like many functional foods, Maitake (*Grifola frondosa*), which is an edible/medicinal mushroom, has been traditionally used for health promotion and longevity in China.[13] Pharmacological studies revealed that the polysaccharide fractions, which were isolated from Maitake, showed multiple physiological and healthy promoting effects including anti-tumor, anti-inflammation and immunomodulation.[14] Among its many biological activities, the immune activity of polysaccharides is recognized as a remarkable feature that can modulate the body's immune functions by regulating immune organs, immune cells and immune molecules.[15] We have reported previously that proteo-β-glucan, a polysaccharide bioactive component of Maitake (PGM), also possessed neuropharmacology activity.[16] Recently, it has been found that the polysaccharides which were extracted from Maitake, could improve cognitive function *via* inhibiting oxidative stress.[17] However, whether PGM could mediate the activation of microglia and improve the AD pathological features, which contributing to its immunomodulatory property, remains unclear.

Therefore, in the present study, we investigated the effects of PGM on cognitive impairment and neuropathology on APP/PS1 mice, an established AD mouse model. Also, we elucidated the underlying cellular and molecular mechanisms of its effects.

Materials and methods

Animals

Male APP/PS1 double-transgenic mice with a C57Bl/6J background were purchased from Model Animal Research Center of Nanjing University (Nanjing, China). They were bred with wild type (WT) C57BL/6J females at School of Medicine, Yunnan University. Offspring were tail-snipped, and genotypes were confirmed by polymerase chain reaction (PCR), using primers specific for the APP sequence of the APP/PS1 construct (forward GACTGACCACTCGACCAGGTTCTG; GTGGATAACCCCTCCCCC AGCCTAGACC; reverse: CTTGTAAGTTGGATTCTCATATCCG; AATAGAGAACGGCAGGAGCA). Offspring males heterozygous for the APP/PS1 transgenic construct were then age-matched with WT littermates, not expressing the transgene, which were used as controls. Both groups of mice were group housed ($n = 4$ per cage) in an animal room and allowed access to food and water *ad libitum*. Animals were maintained on a 12 hour light/dark cycle (lights on/off at 8:00 A.M./20:00 P.M.), within a temperature-controlled room (22 ± 1 °C). All animal procedures were carried out in accordance with the Guide for the Care and Use of Laboratory Animals (ISBN: 0-309-05377-3) and were approved by the Institutional Animal Ethics Committee of Yunnan University (ynucare 20180015).

Preparation of proteo-β-glucan from Maitake (PGM)

The method has been described in our previous literature.[16] Briefly, the Maitake D-fraction was extracted from Maitake mushrooms, which were prepared in a standardized procedure as described previously by Mushroom Wisdom, Inc. The D-fraction obtained using this standard method showed a single peak with a molecule weight of 1200–2000 kDa by HPLC analysis and consisted of 98% polysaccharide and 2% peptides. We purchased the supplies from Mushroom Wisdom Inc (East Rutherford, NJ, USA) and the products are labeled as containing 30% of the D-fraction solution in water and glycerol. We performed a triple volume of 95% ethanol precipitation procedure to remove the water and glycerol. After incubating the mixture for 60 min at room temperature, the samples were centrifuged at 12 000 rcf min^{-1} at 4 °C for 60 min. The precipitate was dried with air and re-dissolved in saline for the animal oral administration. After ethanol extraction, the resulting proteo-β-glucan was defined as the proteo-β-glucan from Maitake (PGM). Next, the mixture was incubated for 1 h at room temperature, and then centrifuged at 12 000 rcf min^{-1} at 4 °C for 1 h. The precipitate was dried with air and re-dissolved in saline for further experiment.

Groups and drug administration

The APP/PS1 mice (6 months-old) and age-matched WT littermates were randomly assigned to the following eight groups ($n = 12$ per group), namely the WT, WT + PGM (5, 10 and 20 mg kg^{-1} per day, respectively), APP/PS1 and APP/PS1 + PGM (5, 10 and 20 mg kg^{-1} per day, respectively) groups.

The mice were intraperitoneal injection of PGM or saline on the morning (between 9:00 A.M. and 11:00 A.M.) for consecutive 3 months in a volume of 10 mL kg^{-1} body weight. Then, the behavioural assessments were conducted once per day for consecutive 7 days. During the period of behavioural assessment, PGM or saline was still administrated to the mice, which lasting for 7 days. All the mice were sacrificed on the second day after the last drug administration (Fig. 1).

Morris water maze (MWM) test

The effect of PGM treatment on the spatial learning and memory abilities of the mice were assessed using the MWM test. Briefly, the maze consisted of a stainless steel pool (120 cm in diameter and 50 cm in height) with a submerged escape-platform (10 cm in diameter) placed 1 cm below the water surface. The water temperature was maintained at 23 ± 1 °C. Mice were randomly placed into one of the four quadrants facing the maze wall and allowed to search for the platform. The time required to find the hidden platform was recorded as the escape latency. The mice were given a maximum of 60 s to find the hidden platform. If the mouse did not find the platform within 60 s, it was guided to the platform and allowed to stay for 3 s, and the maximum escape-latency score of 60 s was assigned. The spatial learning task consisted of six consecutive days of
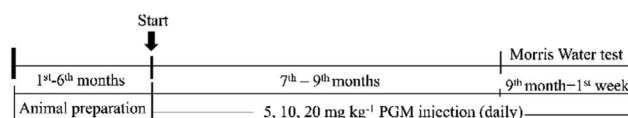

Fig. 1 Schematic representation of the experimental design.

testing, with three trials per day. To test spatial memory, a single probe trial was performed twenty-four hour after the last spatial learning task. The mice were placed into the quadrant opposite to the target quadrant. Mice were allowed to swim freely without the platform for 60 s. The numbers of crossings through this quadrant were recorded.

Preparation of brain sections

Following the behavioral tests, the mice were anesthetized with chloral hydrate (400 mg kg^{-1}) at a volume of 0.1 mL per 10 g body weight and perfused transcardially with phosphate-buffered saline (PBS; Boster, China) for about 20 min followed by 4% cold paraformaldehyde (PFA) in PBS for another 20 min. Brains were fixed in 4% PFA overnight and then immersed in 10%, 20% and 30% sucrose at 4 °C till the brain sank to the bottom for dehydration. Serial coronal sections (5 μm and 20 μm) were cut on a freezing microtome (LEICA CM1950, Germany). All the sections were stored at −80 °C in a specific frozen solution after 1 h baking at a constant 50 °C dryer.

Histological analysis by haematoxylin and eosin staining

The coronal sections (5 μm), which were stored at −80 °C, were kept for 15 min at room temperature. Then, the sections were stained with Mayer's hematoxylin followed by Eosin-Phloxine B. After mounted with coverslips, the bilateral hippocampal dentate gyrus (DG), CA1 and CA3 areas damage were observed under a light microscope (Leica DM2500, Germany).

Nissl staining

For Nissl staining, after keeping at room temperature for 15 min, the sections were rinsed with PBS for 3 min. Then, the sections were immersed in 95% ethanol for 5 min at room temperature followed by immersed in 0.1% Nissl staining solution (Cresyl Fast Violet) (C9140-1g, Cat: G1430, Lot: MKCC9169, Solarbio) for 30 min in an oven at 60 °C. Afterward, sections were mounted for imaging under a light microscope (Leica DM2500, Germany).

Immunohistochemistry

The sections were incubated with 0.3% H_2O_2 in methanol for 10 min to inhibit endogenous peroxidases. After three washed with PBS, the sections were blocked with 10% normal goat serum for 20 min at room temperature, and then incubated with primary antibody anti-A$\beta_{1\text{-}42}$ (1 : 200, 14974, CST, USA) overnight at 4 °C. After washing, the sections were incubated with biotinylated anti-rabbit secondary antibodies (Boster, China) in PBS for 30 min at 37 °C. Then, the sections were incubated with avidinbiotin peroxidase solution (SABC kit, Boster, China) and colorized with a 3,3-diaminobenzidine (DAB) kit (Boster, China). The sections were observed under a light microscope (Leica DM2500, Germany).

Immunofluorescence

Upon use, the sections were rinsed three times with PBST (0.2% Tween-20 in PBS) and blocked with 1% BSA in PBST for 1 h. Then, the sections were incubated with primary antibodies, which included Iba1 (Cat no.: ab5076, Lot: GR237928-2, 1 : 100, Abcam) and GFAP (Cat no.: 12389S, Lot: D1F4Q, 1 : 200, Cell Signaling Technology) overnight at 4 °C. After washing, the sections were incubated with Alexa Fluor 488-conjugated goat anti-mouse IgG (Cat no.: 805-545-180, Lot: 139171, Jackson) or Alexa Fluor 594-conjugated goat anti-rabbit IgG (Cat no.: 711-585-152, Lot: 136429, Jackson) in PBST containing 5% BSA for 1 h at 4 °C, and the nuclear was stained with 4′,6-diamidino-2-phenylindole (DAPI). Then the sections were transferred into a dark box for storage until photograph. Immunofluorescence was visualized using an Olympus Fluo View™ FV1000 confocal microscope.

Image analysis

The sections from each mouse ($n = 5$–8) were selected and digitized by a video camera mounted on a Leica micro-scope (Leica DM2500, Germany). Pictures were further processed using Image-Pro Plus software (version 6.0) and Adobe Photo-shop CS5 (Adobe system). Data were presented by mean value of integrated optical density (IOD) in a total area of 1000 μm × 1000 μm field, and quantified by ImagePro Plus version 6.0 software (Media Cybernetics, Rockville, USA).

Statistical analysis

Results were analyzed using Graph Pad Prism Ver. 5.0 (Graph Pad Software, La Jolla, CA, USA). All data are expressed as mean ± SD. Differences between two groups were analyzed by Student's t-test or nonparametric Mann–Whitney U test and multiple comparisons were assessed by one-way analysis of variance (ANOVA) with Turkey *post hoc* test. Any experimental data value greater than mean plus 2 × standard deviations (SDs) from a group was considered an outlier and was not considered in the analysis. P value < 0.05 was considered statistically significant.

Results

PGM ameliorated learning and memory deficits in APP/PS1 mice

To investigate the potential therapeutic effect of PGM on the cognitive function of APP/PS1 mice, we conducted the MWM test to assess spatial learning and memory ability. Compared with WT mice, the saline-treated APP/PS1 mice spent more time locating the platform (escape latency times) during the training trails (Fig. 2). In addition, the crossing number on the platform in the probe trail was lower in the saline-treated APP/PS1 mice than that of the WT mice. The results indicated that the saline-treated APP/PS1 mice possessed a significantly decreased cognitive ability in terms of spatial learning. Such deficit was improved by PGM treatment, and PGM 10 mg kg^{-1} treatment significantly restored the escape latency in APP/PS1 mice ($P <$ 0.05) (Fig. 2B). Meanwhile, in the probe test, compared with the saline-treated APP/PS1 mice, there was a significantly increased number of platform crossing in PGM treated mice at the dosage of 10 mg kg^{-1} (APP/PS1-PGM 10 mg kg^{-1}) ($P <$ 0.05) (Fig. 2D). These available data suggested that PGM improved the learning
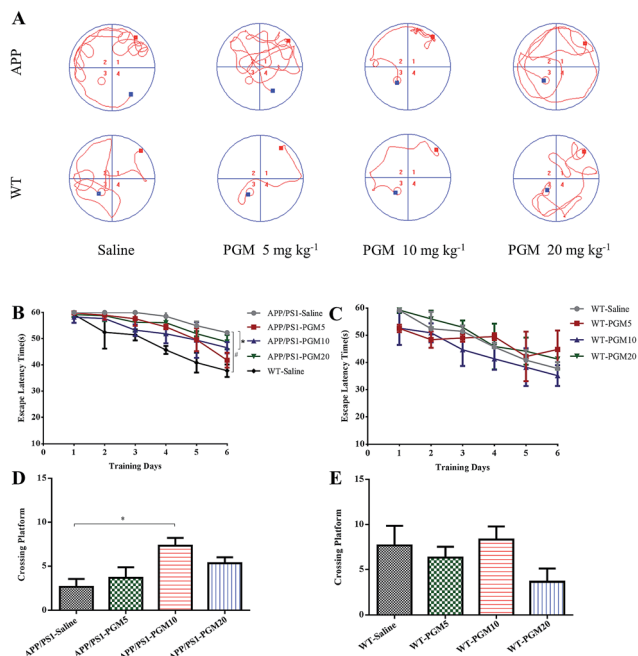
Fig. 2 PGM ameliorated learning and memory deficits in APP/PS1 mice in Morris water maze test. $n = 12$ mice per group. (A) The changes of swimming path. (B and C) The latency to find a hidden platform in APP/PS1 (B) and WT mice (C). (D and E) The number of platform crossing during the spatial probe test in APP/PS1 (D) and WT mice (E). $^{\#}P < 0.05$ vs. WT-saline, $^{*}P < 0.05$ vs. APP/PS1-saline.

Fig. 3 H&E staining of neuronal morphology in hippocampal regions (include DG, CA1 and CA3). (A–C) Representative images of APP/PS1 mice groups. (D and E) Representative images of WT mice groups. Scale bar = 100 μm. $n = 5$–8 mice per group.

and memory ability in APP/PS1 mice. Moreover, there was any significant difference among the WT mice in the escape latency times (Fig. 2C). The results suggested that PGM treatment did not influence the activity of WT mice. In addition, the body weight of all the mice during the experimental period increased slightly, but there was any significant difference in body weight gain among the eight groups (Table 1).

PGM ameliorated histological and morphology of hippocampal area in APP/PS1 mice

Considering the vital role of hippocampal area in the learning and memory, the number and morphology of the hippocampal cells were examined using H&E and Nissl staining. As shown in Fig. 3, the DG, CA1 and CA3 hippocampal cells in the WT mice
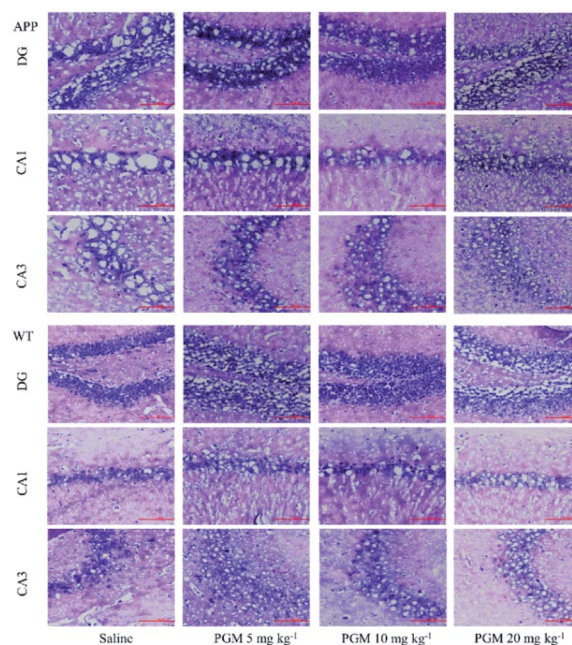
exhibited a regular arrangement with distinct edges and a clear nucleolus and nucleus, and less interstitial space were found as compared with saline-treated APP/PS1 mice. However, a large number of neuronal necrotic cells and injured neurons with an unclear architecture were observed in saline-treated APP/PS1 mice. In addition, the cells were sparse and arranged in disorder with the nucleus pyknotic in this group. Compared with saline-treated APP/PS1 mice, the PGM-treated APP/PS1 mice (5 and 10 mg kg^{-1}) showed an obviously decreased number of necrotic neuron (Fig. 3). The abnormalities of the neuronal morphology were ameliorated by PGM treatment. Moreover, the interstitial space was found to become narrower in PGM-treated APP/PS1 mice as compared with saline-treated APP/PS1 mice (Fig. 3). However, the therapeutic effect of the PGM at the dosage of 20 mg kg^{-1} was not obvious.

The Nissl staining showed that the number of neurons significantly reduced in the hippocampal area in saline-treated

Table 1 Weight changes in each group of mice during the period of PGM treatment. Data are expressed as mean $\pm$ SD ($n = 12$ per group)

|	6th month	6th month + 2nd week	7th month	7th month + 2nd week	8th month	8th month + 2nd week	9th month	9th month + 1st week
APP/PS1-saline	26.57 ± 1.96	26.73 ± 2.59	26.53 ± 2.57	25.6 ± 2.09	25.23 ± 1.95	25.25 ± 2.93	25.56 ± 1.85	25.85 ± 2.01
APP/PS1-PGM 5	29.06 ± 3.14	28.68 ± 3.28	28.72 ± 3.27	28.72 ± 3.10	28.86 ± 3.00	29.82 ± 3.14	30.94 ± 3.68	31.44 ± 3.46
APP/PS1-PGM 10	28.97 ± 3.87	28.49 ± 3.83	29.18 ± 3.78	27.83 ± 3.39	28.31 ± 4.29	27.84 ± 3.38	30.46 ± 3.58	31.33 ± 4.09
APP/PS1-PGM 20	28.03 ± 4.30	27.25 ± 3.92	27.14 ± 4.03	27.87 ± 3.89	28.02 ± 3.87	27.89 ± 3.75	28.96 ± 4.17	29.16 ± 4.16
WT-saline	27.34 ± 3.71	26.81 ± 3.18	26.00 ± 3.14	26.37 ± 2.99	26.05 ± 3.19	26.09 ± 3.50	26.15 ± 2.16	26.02 ± 1.95
WT-PGM 5	29.11 ± 3.22	28.35 ± 3.45	28.43 ± 3.07	28.55 ± 2.96	27.86 ± 2.86	28.04 ± 2.40	28.6 ± 2.48	28.57 ± 2.40
WT-PGM 10	29.00 ± 2.27	28.62 ± 2.27	28.05 ± 1.93	27.99 ± 1.99	27.36 ± 2.26	28.06 ± 2.08	29.06 ± 2.05	29.21 ± 2.08
WT-PGM 20	28.91 ± 1.78	27.52 ± 2.10	27.64 ± 2.43	28.09 ± 1.92	27.97 ± 1.90	28.39 ± 1.96	29.07 ± 1.97	29.43 ± 1.55
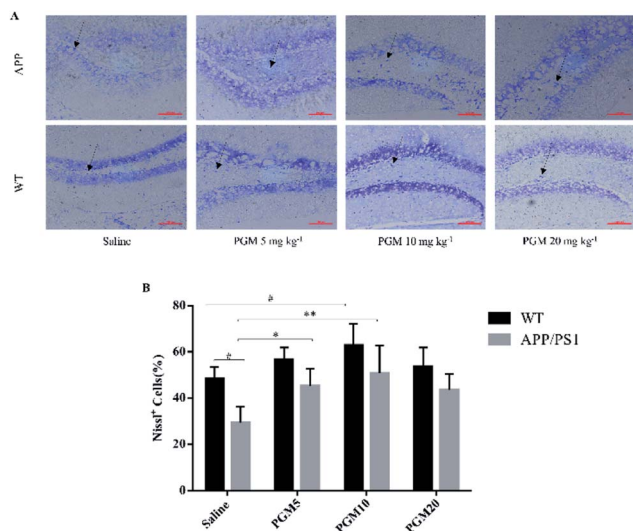
Fig. 4 Nissl staining of neuronal morphology in hippocampal DG region. (A) Representative light micrographs of Nissl-stained DG hippocampal cells. Scale bar = 100 μm. (B) Quantitative analysis of Nissl cells in the DG regions of the hippocampus. n = 5–8 mice per group. [#]$P < 0.05$ vs. WT-saline, *$P < 0.05$ vs. APP/PS1-saline, **$P < 0.01$ vs. APP/PS1-saline.

APP/PS1 mice as compared with WT mice (Fig. 4). The results obtained from Nissl staining were in consistent with the above-mentioned results. While after being treated with PGM, the distorted hippocampal cell morphology was attenuated and the number of Nissl bodies were increased significantly (Fig. 4). Apparently, the reduction in the number of neurons was significantly lower in the PGM 5 and 10 mg kg^{-1} treated APP/PS1 mice as compared with saline-treated APP/PS1 mice ($P < 0.05$ and $P < 0.01$, respectively) (Fig. 4B). In addition, compared with saline-treated APP/PS1 mice, the PGM-treated (5 and 10 mg kg^{-1}) APP/PS1 mice showed significantly ameliorated abnormalities of neuronal morphology. These available data indicated that PGM could ameliorate the abnormalities of hippocampal region in APP/PS1 mice and possessed protective effect on the morphology of hippocampal neurons.

PGM alleviated Aβ plaque burden in APP/PS1 mice

Then, we explored whether PGM exerted its effect on alleviation of Aβ pathology. To examine the amyloid burden in APP/PS1 mice, the immunostaining with the anti-Aβ$_{1-42}$ antibody was performed in the brain sections, and the amount of Aβ$_{1-42}$ plaques was quantified. Compared with WT mice, the APP/PS1 mice showed a significantly higher of the mean area covered by Aβ$_{1-42}$-positive plaques in the cortex and hippocampal region (include DG, CA1 and CA3) (Fig. 5A–D). While, the mean area containing Aβ plaques was significantly less in PGM-treated APP/PS1 mice than that of the saline-treated APP/PS1 mice (Fig. 5E–H). The results demonstrated that PGM significantly reduced the plaque number per mm^2 of Aβ$_{1-42}$-positive plaques compared with the saline-treated APP/PS1 mice, suggesting that PGM exerted its effect on alleviation of Aβ pathology.

PGM aggrandized glial cell activation in the hippocampal region in APP/PS1 mice

Glia cells, which are abundant cell types found in the central nervous system, have been shown to play crucial roles in regulating both normal and disease states especially in AD pathology.[18] To investigate the effect of PGM on the activation of glial, the astrocyte marker (GFAP) and microglial marker (Iba1) expression were determined using immunofluorescent staining in the hippocampal DG region of APP/PS1 mice (Fig. 6A–D). Compared to saline-treated APP/PS1 mice, PGM treated APP/PS1 mice at the dosage of 10 mg kg^{-1} showed a significantly increased number of the activated astrocytes and microglia in the hippocampal DG ($P < 0.01$ and $P < 0.05$, respectively) (Fig. 6E and G). In addition, the size of the activated astrocytes and microglia in the hippocampal DG was enlarger than that of the saline-treated APP/PS1 mice (Fig. 6A and C). While there was no significant differences in PGM treated mice at the dosage of 5 and 20 mg kg^{-1} groups. However, in WT mice, there was any significant difference between the PGM treated mice and the saline-treated mice in glia cell activation (Fig. 6F and H).
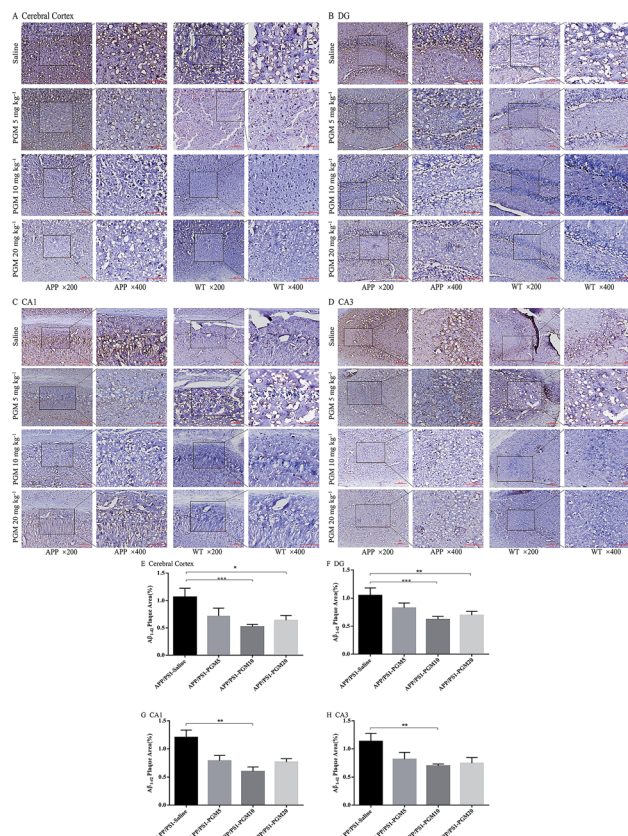

Fig. 5 PGM alleviated brain Aβ$_{1-42}$ burden in APP/PS1 mice. (A–D) Respectively representative images of Aβ$_{1-42}$ deposits in the cerebral cortex and the DG, CA1, CA3 regions of the hippocampus. Scale bar = 100 μm. (E–H) Respectively quantification of Aβ$_{1-42}$ area in the cerebral cortex and the DG, CA1, CA3 regions of the hippocampus. n = 5–8 mice per group, three sections per animal. *$P < 0.05$ vs. APP/PS1-saline, **$P < 0.01$ vs. APP/PS1-saline, ***$P < 0.001$ vs. APP/PS1-saline.
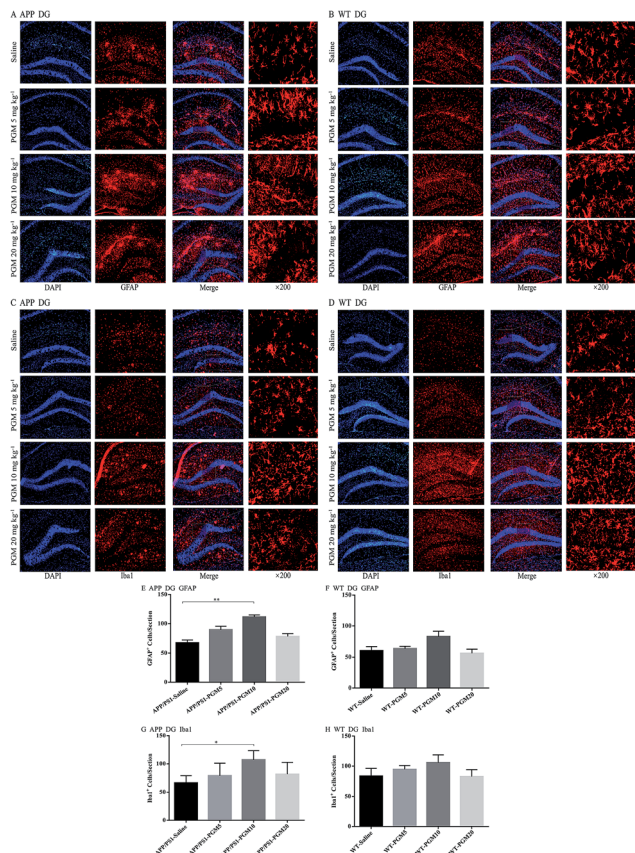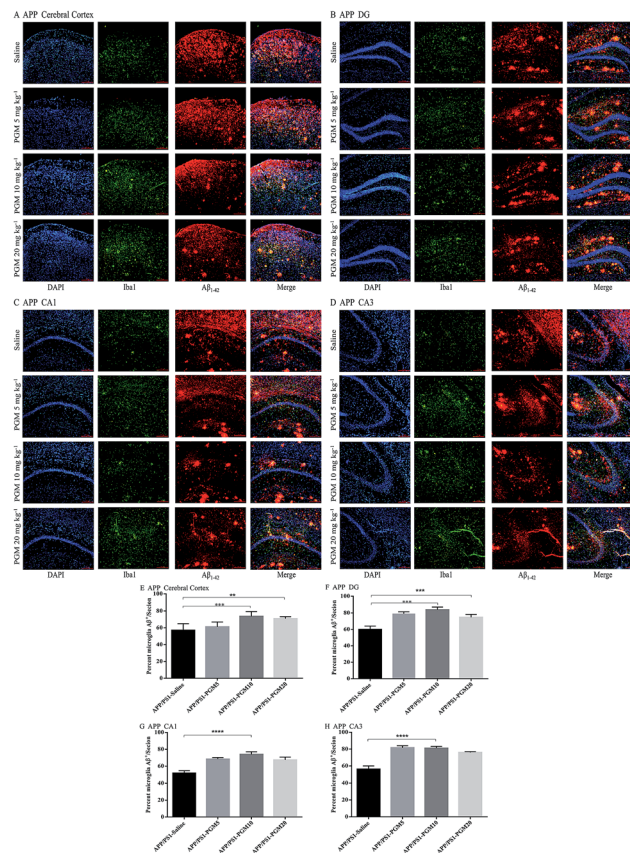
Fig. 6 PGM aggrandized glial cell activation in the hippocampal regions of APP/PS1 mice. (A) Fluorescent GFAP (red)/DAPI (blue) colocalization in the DG regions of the hippocampus in APP/PS1 mice. Scale bar = 100 μm. (B) Fluorescent GFAP (red)/DAPI (blue) colocalization in the DG regions of the hippocampus in WT mice. Scale bar = 100 μm. (C) Fluorescent Iba1 (red)/DAPI (blue) colocalization in the DG regions of the hippocampus in APP/PS1 mice. Scale bar = 100 μm. (D) Fluorescent Iba1 (red)/DAPI (blue) colocalization in the DG regions of the hippocampus in WT mice. Scale bar = 100 μm. (E) Quantification of GFAP-positive cells in each APP/PS1 mice group. $n = 5-8$ per group, three sections per animal. (F) Quantification of GFAP-positive cells in each WT mice group. $n = 5-8$ per group, three sections per animal. (G) Quantification of Iba1-positive cells in each APP/PS1 mice group. $n = 5-8$ per group, three sections per animal. (H) Quantification of Iba1-positive cells in each WT mice group, $n = 5-8$ per group, three sections per animal. $*P < 0.05$ vs. APP/PS1-saline, $**P < 0.01$ vs. APP/PS1-saline.

Fig. 7 PGM aggrandized glial cell activation and increased amyloid endocytosis by microglia in the hippocampal regions of APP/PS1 mice. (A–D) Fluorescent $A\beta_{1-42}$ (red)/Iba1 (green)/DAPI (blue) colocalization in the cortex (A) and the DG (B), CA1 (C), CA3 (D) regions of the hippocampus in APP/PS1 mice. Scale bar = 100 μm. (E–H) Percentage of Iba1-positive microglia cell bodies that are also Aβ-positive in the cortex (E) and the DG (F), CA1 (G) and CA3 (H) regions of the hippocampus. $n = 5-8$ mice per group, three sections per animal. $**P < 0.01$ vs. APP/PS1-saline, $***P < 0.001$ vs. APP/PS1-saline, $****P < 0.0001$ vs. APP/PS1-saline.

PGM enhanced microglial recruitment around the plaques and promoted Aβ phagocytosis and clearance

Microglia are macrophage-like phagocytes in the central nervous system.[6] In the brain, extracellular Aβ is mainly phagocytosed and cleared by microglia.[18] Given that the significant reduction of Aβ deposits was found in APP/PS1 mice upon PGM treatment, the immunochemistry analysis was performed to co-label microglia and Aβ plaques using anti-Iba1 and anti-$A\beta_{1-42}$ antibodies. The results showed that microglia were recruited adjacent to the plaques in the cortex and hippocampal region (include DG, CA1 and CA3) in APP/PS1 mice (Fig. 7A–D). The recruitment of microglia surrounding $A\beta_{1-42}$ plaques was significantly enhanced by PGM treatment. The percentage of microglia and Aβ plaque

burden overlap in these areas were determined by optical density analysis. Apparently, an increased percentage of co-labeled microglia in cortex (73.65% ± 2.5%), DG (83.8% ± 1.51%), CA1 (73.96% ± 1.41%) and CA3 (81.07% ± 0.98%) was observed in PGM 10 mg kg^{-1} treated mice as compared with saline-treated APP/PS1 mice (Fig. 7E–H). The results suggested that PGM decreased the Aβ plaque burden via promoting the activation of microglia cells, which clustered around the Aβ plaque burden, and thereby performed the corresponding role of phagocytosis and clearance.

Discussion

In past decades, great efforts have been made to investigate the pathogenesis and therapies of AD. Current medications used to treat AD, which include donepezil and memantine, are not highly effective.[19] Therefore, further investigation into the effective interventions which could counteract AD is needed. Recently, owing to their multimodal effects and relatively low

toxicities, the functional foods are become highly potent drug candidates for the treatment of AD.[20] In the present study, we revealed that a polysaccharide bioactive component of Maitake (PGM) could significantly alleviate learning and memory deficits in APP/PS1 mice. The present findings highlighted the possibility of using PGM as a drug for the treatment of AD.

Maitake (*Grifola frondosa*), the king of mushrooms, is one of the most valuably traditional medicines. It has been used as a health food for a long time in China, Japan, and other Asian countries.[15] Polysaccharides, which were extracted from Maitake, have been reported to possess multiple effects such as immunomodulatory, antitumor and antioxidant effects.[14] In a recent study, Chen *et al.* reported that oral administration of *Grifola frondosa* polysaccharides could improve memory impairment *via* antioxidant action in aged rats.[17] Such polysaccharides exerted their biological activities mainly through immunomodulation, however, whether the polysaccharides improved the learning and memory ability through mediating the immune pathway remains unclear. In addition, the role of PGM in Aβ deposition, the most iconic pathological marker of AD, remains unexplored. Nowadays, APP/PS1 double transgenic mice, which mimic the pathological hallmarks of AD in terms of Aβ deposition, have been widely used as an animal model of AD.[21] This study further suggested that PGM could improve the learning and memory impairment in APP/PS1 mice, and provided clear evidence that PGM treatment could increase the number of surviving neurons and maintain the histomorphology of the hippocampus. Moreover, PGM could enhance microglial recruitment adjacent to the Aβ plaques and improve microglial phagocytic capacity, and thereby promoted Aβ clearance in APP/PS1 mice.

In concert with the behavioural result, H&E and Nissl staining revealed that the neuronal cells of cortex and hippocampus of APP/PS1 mice were significantly loss and shrinkage than those of the WT mice. The changes of neuronal cell density and morphology were in consistent with the previous study that a number of pathological modifications were observed in the brain of APP/PS1 mice.[19,22] In the current study, the reduction of the shrunken neurons and ameliorative cell morphology were found by PGM (5 and 10 mg kg^{-1}) treatment, indicating that PGM possessed a neuroprotective effect. Moreover, the Nissl positive cell numbers per mm^2 in the DG region of the hippocampus in PGM (5 and 10 mg kg^{-1}) treated mice showed a significant increase as compared with saline treated-APP/PS1 mice. The results indicated that PGM could protect neurons from damage, and thereby improved the learning and memory impairment.

It has been reported that the accumulation and deposition of Aβ in the brain could drive the pathogenic cascades of AD.[1] Microglia, the resident immune cells of the brain, are the first responders to Aβ accumulation and phagocytosis.[23] During the disease progression of AD, microglia cluster around Aβ deposits and adopt a polarized morphology with hypertrophic processes extending toward plaques.[18] Microglia exerted the potentially protective impact on AD progression through regulating the degree of amyloid deposition by phagocytosis of amyloid aggregates.[24] Recently, it is reported that multi-sensory gamma

stimulation can ameliorate Alzheimer's-associated pathology and improves cognition, enhancing microglial recruitment around the plaques and promoting of the Aβ phagocytosis and clearance played important roles in this process.[25] Moreover, Zhao *et al.* reported that depletion of microglia in an AD mouse model led to an overproduction of plaque. Also, dendritic spine loss and shaft atrophy in adjacent neurons were observed in AD mouse model.[26] However, chronic and sustained microglial activation could cause the overproduction of neurotoxic inflammatory cytokines and reactive oxygen species, which aggravated the disease progression of AD.[27] Unfortunately, AD patients who accepted anti-inflammatory therapy did not show any cognitive benefits,[28] suggesting that neuroinflammation was not a major driver of AD. Actually, inflammation in neurodegenerative disease is a double-edged sword.[29] Therefore, we thought that the activated status of glial cells and their roles in the pathology of AD were related to the disease progression of AD and the type, intensity and duration of the medication used to treat AD. Thus, the specific mechanisms and the corresponding outcomes should be explored.

Furthermore, several evidences showed that a β-glucan, which was extracted from *Grifola frondosa*, not only directly activated various immune effector cells (macrophages, killer T cells, and natural killer cells), but also potentiated the activities of various mediators, including lymphokines and IL-1 (the first mediator in the activation of T cell lines).[14] Remarkably, polysaccharides derived from *Grifola frondosa* were more likely to activate the immune system under pathological condition, and thereby exerted multiple biological activities. However, like most immunomodulators, PGM showed a double-edged sword effect on the regulation and subsequent effect of immunity; it has a beneficial effect with reasonable concentration and intensity, otherwise it might be difficult to exert its effect or show adverse effect. In the current study, the results suggested that PGM possessed the most satisfactory effect on the learning ability of APP/PS1 mice and the most significantly protective effect on hippocampus at the medium dosage (10 mg kg^{-1}). In addition, the clearance of Aβ deposits and regulation of glial cells were most effective by PGM treatment at this dosage. While, the high dosage of PGM (20 mg kg^{-1}) did not show the above effects. Therefore, the follow-up study of PGM especially the dose-effect relationship on glial cells and the corresponding role in AD should be applied. In addition, it is imperative to study the therapeutic basis of PGM, including exploring whether there are other immune effector molecules and key signalling pathways are involved.

Conclusions

In summary, our results demonstrated that PGM, a protein-bound polysaccharide bioactive component of Maitake, could ameliorate the learning and memory function and histopathological abnormalities in hippocampal region in APP/PS1 mice. The activation of microglia and astrocytes and promotion of microglial recruitment to the plaques and enhancement of Aβ phagocytosis were found by PGM treatment. These effects were contributed to the alleviation of Aβ burden and the pathological

changes in the hippocampus and cortex. Meanwhile, we did not observe any abnormalities or toxicity in mice by chronic or acute use of PGM. Therefore, PGM maybe a promising new candidate drug for the treatment of AD.

Conflicts of interest

There are no conflicts to declare.

Acknowledgements

References

1 R. Y. Pan, J. Ma, X. X. Kong, X. F. Wang, S. S. Li, X. L. Qi, Y. H. Yan, J. Cheng, Q. Liu, W. Jin, C. H. Tan and Z. Yuan, Sodium rutin ameliorates Alzheimer's disease-like pathology by enhancing microglial amyloid-beta clearance, *Sci. Adv.*, 2019, **5**, eaau6328.

2 D. Zhu, N. Yang, Y. Y. Liu, J. Zheng, C. Ji and P. P. Zuo, M2 Macrophage Transplantation Ameliorates Cognitive Dysfunction in Amyloid-beta-Treated Rats Through Regulation of Microglial Polarization, *J. Alzheimer's Dis.*, 2016, **52**, 483–495.

3 M. T. Heneka, D. T. Golenbock and E. Latz, Innate immunity in Alzheimer's disease, *Nat. Immunol.*, 2015, **16**, 229–236.

4 J. Hardy and D. J. Selkoe, The amyloid hypothesis of Alzheimer's disease: progress and problems on the road to the rapeutics, *Science*, 2002, **297**, 353–356.

5 L. Mucke and D. J. Selkoe, Neurotoxicity of amyloid beta-protein: synaptic and network dysfunction, *Cold Spring Harbor Perspect. Med.*, 2012, **2**, a006338.

6 C. Condello, P. Yuan and J. Grutzendler, Microglia-Mediated Neuroprotection, TREM2, and Alzheimer's Disease: Evidence From Optical Imaging, *Biol. Psychiatry*, 2018, **83**, 377–387.

7 C. Y. Lee and G. E. Landreth, The role of microglia in amyloid clearance from the AD brain, *J. Neural Transm.*, 2010, **117**, 949–960.

8 M. Ries and M. Sastre, Mechanisms of Abeta Clearance and Degradation by Glial Cells, *Front. Aging Neurosci.*, 2016, **8**, 160.

9 H. Lian, A. Litvinchuk, A. C. Chiang, N. Aithmitti, J. L. Jankowsky and H. Zheng, Astrocyte-Microglia Cross Talk through Complement Activation Modulates Amyloid Pathology in Mouse Models of Alzheimer's Disease, *J. Neurosci.*, 2016, **36**, 577–589.

10 E. Huh, S. Lim, H. G. Kim, S. K. Ha, H. Y. Park, Y. Huh and M. S. Oh, Ginger fermented with Schizosaccharomyces pombe alleviates memory impairment *via* protecting hippocampal neuronal cells in amyloid beta$_{1-42}$ plaque injected mice, *Food Funct.*, 2018, **9**, 171–178.

11 H. G. Kim and M. S. Oh, Herbal medicines for the prevention and treatment of Alzheimer's disease, *Curr. Pharm. Des.*, 2012, **18**, 57–75.

12 N. Nillert, W. Pannangrong, J. U. Welbat, W. Chaijaroonkhanarak, K. Sripanidkulchai and B. Sripanidkulchai, Neuroprotective Effects of Aged Garlic Extract on Cognitive Dysfunction and Neuroinflammation Induced by beta-Amyloid in Rats, *Nutrients*, 2017, **9**, E24.

13 Y. W. Tsao, Y. C. Kuan, J. L. Wang and F. Sheu, Characterization of a novel maitake (*Grifola frondosa*) protein that activates natural killer and dendritic cells and enhances antitumor immunity in mice, *J. Agric. Food Chem.*, 2013, **61**, 9828–9838.

14 X. He, X. Wang, J. Fang, Y. Chang, N. Ning, H. Guo, L. Huang, X. Huang and Z. Zhao, Polysaccharides in *Grifola frondosa* mushroom and their health promoting properties: a review, *Int. J. Biol. Macromol.*, 2017, **101**, 910–921.

15 M. Meng, M. Guo, C. Feng, R. Wang, D. Cheng and C. Wang, Water-soluble polysaccharides from *Grifola frondosa* fruiting bodies protect against immunosuppression in cyclophosphamide-induced mice *via* JAK2/STAT3/SOCS signal transduction pathways, *Food Funct.*, 2019, **10**, 4998–5007.

16 H. Bao, P. Ran, M. Zhu, L. Sun, B. Li, Y. Hou, J. Nie, L. Shan, H. Li, S. Zheng, X. Xu, C. Xiao and J. Du, The Prefrontal Dectin-1/AMPA Receptor Signaling Pathway Mediates The Robust and Prolonged Antidepressant Effect of Proteo-beta-Glucan from Maitake, *Sci. Rep.*, 2016, **6**, 28395.

17 Z. Chen, Y. Tang, A. Liu, X. Jin, J. Zhu and X. Lu, Oral administration of *Grifola frondosa* polysaccharides improves memory impairment in aged rats *via* antioxidant action, *Mol. Nutr. Food Res.*, 2017, **61**, DOI: 10.1002/mnfr.201700313.

18 C. Condello, P. Yuan, A. Schain and J. Grutzendler, Microglia constitute a barrier that prevents neurotoxic protofibrillar Abeta42 hotspots around plaques, *Nat. Commun.*, 2015, **6**, 6176.

19 C. Yuan, X. Guo, Q. Zhou, F. Du, W. Jiang, X. Zhou, P. Liu, T. Chi, X. Ji, J. Gao, C. Chen, H. Lang, J. Xu, D. Liu, Y. Yang, S. Qiu, X. Tang, G. Chen and L. Zou, OAB-14, a bexarotene derivative, improves Alzheimer's disease-related pathologies and cognitive impairments by increasing beta-amyloid clearance in APP/PS1 mice, *Biochim. Biophys. Acta, Mol. Basis Dis.*, 2019, **1865**, 161–180.

20 J. S. Ha, J. M. Kim, S. K. Park, J. Y. Kang, D. S. Lee, U. Lee, D. O. Kim, S. G. Choi and H. J. Heo, Anti-amyloidogenic properties of an ethyl acetate fraction from Actinidia arguta in Abeta$_{1-42}$-induced ICR mice, *Food Funct.*, 2018, **9**, 3264–3277.

21 S. Jo, O. Yarishkin, Y. J. Hwang, Y. E. Chun, M. Park, D. H. Woo, J. Y. Bae, T. Kim, J. Lee, H. Chun, H. J. Park, D. Y. Lee, J. Hong, H. Y. Kim, S. J. Oh, S. J. Park, H. Lee, B. E. Yoon, Y. Kim, Y. Jeong, I. Shim, Y. C. Bae, J. Cho, N. W. Kowall, H. Ryu, E. Hwang, D. Kim and C. J. Lee, GABA from reactive astrocytes impairs memory in mouse models of Alzheimer's disease, *Nat. Med.*, 2014, **20**, 886–896.

22 Z. Gong, J. Huang, B. Xu, Z. Ou, L. Zhang, X. Lin, X. Ye, X. Kong, D. Long, X. Sun, X. He, L. Xu, Q. Li and A. Xuan, Urolithin A attenuates memory impairment and neuroinflammation in APP/PS1 mice, *J. Neuroinflammation*, 2019, **16**, 62.

23 W. J. Streit, H. Braak, K. D. Tredici, J. Leyh, J. Lier, H. Khoshbouei, C. Eisenlöffel, W. Müller and I. Bechmann, Microglial activation occurs late during preclinical Alzheimer's disease, *Glia*, 2018, **66**, 2550–2562.

24 M. Ries and M. Sastre, Mechanisms of Abeta Clearance and Degradation by Glial Cells, *Front. Aging Neurosci.*, 2016, **8**, 160.

25 A. J. Martorell, A. L. Paulson, H. J. Suk, F. Abdurrob, G. T. Drummond, W. Guan, J. Z. Young, D. N. Kim, O. Kritskiy, S. J. Barker, V. Mangena, S. M. Prince, E. N. Brown, K. Chung, E. S. Boyden, A. C. Singer and L. H. Tsai, Multi-sensory Gamma Stimulation Ameliorates Alzheimer's-Associated Pathology and Improves Cognition, *Cell*, 2019, **177**, 256–271.

26 R. Zhao, W. Hu, J. Tsai, W. Li and W. B. Gan, Microglia limit the expansion of beta-amyloid plaques in a mouse model of Alzheimer's disease, *Mol. Neurodegener.*, 2017, **12**, 47.

27 M. L. Block, L. Zecca and J. S. Hong, Microglia-mediated neurotoxicity: uncovering the molecular mechanisms, *Nat. Rev. Neurosci.*, 2007, **8**, 57–69.

28 P. S. Aisen, The potential of anti-inflammatory drugs for the treatment of Alzheimer's disease, *Lancet Neurol.*, 2002, **1**, 279–284.

29 T. Wyss-Coray and L. Mucke, Inflammation in neurodegenerative disease – a double-edged sword, *Neuron*, 2002, **35**, 419–432.